EC
Journals.ASM.org

The Transcriptional Response of *Cryptococcus neoformans* to Ingestion by *Acanthamoeba castellanii* and Macrophages Provides Insights into the Evolutionary Adaptation to the Mammalian Host

Lorena da S. Derengowski,[a,b] Hugo Costa Paes,[a] Patrícia Albuquerque,[a,b] Aldo Henrique F. P. Tavares,[a,c] Larissa Fernandes,[a,c] Ildinete Silva-Pereira,[a] Arturo Casadevall[b]

Laboratório de Biologia Molecular, CEL/IB, Universidade de Brasília, Brasília, DF, Brazil[a]; Albert Einstein College of Medicine of Yeshiva University, Bronx, New York, USA[b]; Faculdade de Ceilândia, FCE/UnB, Universidade de Brasília, Brasília, DF, Brazil[c]

Virulence of *Cryptococcus neoformans* for mammals, and in particular its intracellular style, was proposed to emerge from evolutionary pressures on its natural environment by protozoan predation, which promoted the selection of strategies that allow intracellular survival in macrophages. In fact, *Acanthamoeba castellanii* ingests yeast cells, which then can replicate intracellularly. In addition, most fungal factors needed to establish infection in the mammalian host are also important for survival within the amoeba. To better understand the origin of *C. neoformans* virulence, we compared the transcriptional profile of yeast cells internalized by amoebae and murine macrophages after 6 h of infection. Our results showed 656 and 293 genes whose expression changed at least 2-fold in response to the intracellular environments of amoebae and macrophages, respectively. Among the genes that were found in both groups, we focused on open reading frame (ORF) CNAG_05662, which was potentially related to sugar transport but had no determined biological function. To characterize its function, we constructed a mutant strain and evaluated its ability to grow on various carbon sources. The results showed that this gene, named *PTP1* (polyol transporter protein 1), is involved in the transport of 5- and 6-carbon polyols such as mannitol and sorbitol, but its presence or absence had no effect on cryptococcal virulence for mice or moth larvae. Overall, these results are consistent with the hypothesis that the capacity for mammalian virulence originated from fungus-protozoan interactions in the environment and provide a better understanding of how *C. neoformans* adapts to the mammalian host.

Cryptococcus neoformans is an opportunistic pathogen often found in soils contaminated with bird excreta (1). Infection by *C. neoformans*, which occurs through inhalation of propagules from the environment by the host, seems to be accidental since *C. neoformans* is a saprophytic fungus that does not require an animal host for replication and survival (2). In the case of human exposure to *C. neoformans*, the establishment of infection and subsequent development of cryptococcosis depend both on the host's immune response and the virulence of the fungus (3) One of the first lines of defense in the lung are alveolar macrophages, which are able to phagocytose *C. neoformans* efficiently (4). Phagocytosis is followed by phagosome acidification and fusion of lysosomes (5). However, this process does not always result in the death of yeast cells and *C. neoformans* can survive and replicate within macrophages *in vivo*, as shown by Feldmesser et al. (6).

The ability of *C. neoformans* to survive in the intracellular environment of phagocytes might have a critical role in disease progression and probably contributes to the propensity of the fungus to cause chronic and latent infections (3, 7, 8). However, it is known that the intracellular microenvironment of phagocytes is extremely inhospitable to internalized microorganisms due to nutritional and oxidative stress and exposure to antimicrobial peptides and hydrolytic enzymes (9, 10, 11). To survive the harsh environment of the phagosome, *C. neoformans* is able to reprogram its gene expression profile. Twenty-four hours after phagocytosis by murine macrophages, *C. neoformans* responds to carbon starvation by upregulating genes that encode sugar transporters and proteins involved in the utilization of alternative carbon sources, including enzymes of the glyoxylate cycle and fatty acid metabolism. Genes related to the oxidative stress response were also induced (4).

Since *C. neoformans* is a free-living fungus, its mammalian intracellular lifestyle is particularly curious, given that this organism has no obvious requirement for animal virulence in its life cycle. In this sense, the evolutionary origin and the maintenance of virulence strategies that allow for survival of *C. neoformans* within macrophages have been an issue of interest, and the investigation of the *C. neoformans* ecological niche may be informative in this regard. Steenbergen et al. (12) suggested that the competence of *C. neoformans* to proliferate within mammalian phagocytic cells was initially selected to confer an advantage against environmental predators. This idea was supported by the fact that interaction of *C. neoformans* with the amoeba *Acanthamoeba castellanii* results in the ingestion of the fungus followed by its intracellular replication and the accumulation of vesicles containing polysaccharide in the cytoplasm of amoeboid cells (12). This result is similar to those previously observed in the interaction of *C. neoformans* with macrophages. Furthermore, mutant strains defective in capsule

Received 18 March 2013 **Accepted** 19 March 2013
Published ahead of print 22 March 2013
Address correspondence to Lorena da S. Derengowski, lorena.bio@gmail.com.
I.S.-P. and A.C. share senior authorship of this article.
Supplemental material for this article may be found at http://dx.doi.org/10.1128/EC.00073-13.

doi:10.1128/EC.00073-13

and phospholipase production, two important virulence factors of *C. neoformans*, are unable to survive within *A. castellanii* (12), indicating that virulence factors known to be required for the persistence of the fungus in animals can also be required for persistence in environmental predators (13, 14). Additional supportive data for this hypothesis came from the interaction of *C. neoformans* with the free-living slime mold *Dictyostelium discoideum*, which significantly increases the virulence of the fungus in a murine model of infection (15). Thus, it has been postulated that the intracellular survival strategy used by *C. neorfomans* in mammalian macrophages is a consequence of evolutionary selection for fungus survival within soil protozoa.

We hypothesize that this adaptive convergence is a result of the similarity between the intracellular environments of macrophages and amoebae. Consequently, we have compared the transcriptional profiles of *C. neoformans* after 6 h of interaction with *A. castellanii* or murine macrophages. Our results suggest a conserved metabolic response of *C. neoformans* to the microenvironments of both cells.

MATERIALS AND METHODS

Cell lines and media. The H99 strain of *C. neoformans* var. *grubii* (serotype A) was used as the wild-type strain for microarray experiments. The *C. neoformans* serotype A strain KN99α was used to generate the ptp1Δ mutant and the ptp1Δ::ptp1 complemented strains for the CNAG_05662 open reading frame (ORF). We also used the D1307 mutant strain depleted for the CNAG_05662 reading frame obtained from a *C. neoformans* mutant library (16) purchased from ATCC. All strains were maintained at −80°C. Cultures were initiated by streaking YPD agar plates (containing 1% yeast extract, 2% Bacto peptone, and 2% dextrose [pH 6.8]) and incubating them for 2 days at 30°C, followed by seeding a single colony in YPD liquid medium and incubating it at 30°C overnight with agitation. The murine macrophage line J774A.1 was maintained at 37°C in 5% CO_2 in Dulbecco's modified Eagle's medium (DMEM) (11965; GibcoBRL) supplemented with 10% heat-inactivated fetal calf serum (Gibco BRL), 10% NCTC-109 medium (GibcoBRL; 21340) and 1% nonessential amino acids (GibcoBRL; 11140). The *Acanthamoeba castellanii* 30234 strain (ATCC) was maintained in the dark at 28°C on PYG medium (2% peptone, 0.1% yeast extract, 1.8% glucose [pH 7.2]).

Phagocytosis assay. Approximately 1×10^5 cells of the J774A.1 macrophage line or 2×10^5 cells of *A. castellanii* were added to each well of 96-well tissue culture plates with 200 μl/well of DMEM or PYG medium, respectively. Amoebae and macrophages were cultured for 18 h at 28°C and 37°C in 5% CO_2, respectively. Subsequently, the culture supernatant was removed, the remaining cells were washed with sterile 1× phosphate-buffered saline (PBS), and 1×10^6 yeast cells of *C. neoformans* were added to each well. In both cases, the effector-to-target ratio was about 5:1. For macrophage infections, the monoclonal antibody (MAb) 18B7 was included at 10 μg/ml as an opsonin. The cocultures of *C. neoformans* with amoebae or macrophages were then incubated for 15 min, 30 min, 1 h, 2 h, 4 h, or 6 h at 28 or 37°C, respectively, in 5% CO_2. At each time, the culture supernatant was discarded and wells were washed, fixed with cold methanol, and stained with Giemsa. Using optical microscopy, 100 to 200 cells of amoebae or macrophages were counted per well to determine the percentage of phagocytosis at each interval postinfection. The experiments were performed in quadruplicate. GraphPad Prism 5.0 (GraphPad Software) was used for statistical analyses. The paired two-tailed Student's *t* test was used, and a *P* value of ≤0.05 was considered significant. In addition, multiple group comparisons were conducted by one-way analysis of variance (ANOVA) followed by the Bonferroni's correction, as appropriate.

RNA preparation. For the microarray analysis, *C. neoformans* yeast cells were grown in YPD for 24 h at 30°C. The cells were harvested by centrifugation, washed twice with 1× PBS, and counted using a hemocytometer. Amoebae and macrophages were each grown in 175-cm^2 culture flasks (BD Molecular Biotechnology) with 75 ml of PYG medium or DMEM, respectively, until near confluence. H99 yeast cells were added to each flask at an approximate effector-to-target ratio of 5:1 (10^8 yeast cells/flask). For macrophage infection, the MAb 18B7 was added at 10 μg/ml. Flasks were incubated for 6 h at 37°C in 5% CO_2 (macrophages) or 28°C (amoebae). As controls, H99 cells were cultured *in vitro* in the same medium under the same temperature and incubation conditions as the macrophage and amoeba cocultures. At 6 h postinfection, extracellular *C. neoformans* cells and detached phagocytic cells were rinsed off with 1× PBS, and attached amoebae and macrophages were lysed by the addition of 25 mM deoxycholate. This treatment preserves fungal cells (data not shown). Yeast cells were recovered by centrifugation and used for total RNA extraction with TRIzol reagent (Invitrogen) following the manufacturer's recommendations. To minimize contamination with genomic DNA, total RNA was further purified with the RNAeasy kit (Qiagen). The concentration and purity of total RNA were assessed by measuring the 260/280-nm absorbance ratio, and its quality was determined by an Agilent 2100 bioanalyzer (Agilent Technologies) according to the manufacturer's recommendations.

Microarray. The microarray assay was performed by the Genome Technology Access Center (GTAC) at Washington University in St. Louis (https://gtac.wustl.edu). First-strand cDNA was generated by oligo(dT)-primed reverse transcription (Superscript II; Invitrogen) utilizing the 3DNA Array 350 kit (Genisphere). Modified oligo-dT primers were utilized in which a fluorophore/dendrimer-specific oligonucleotide sequence was attached to the 5′ end of the dT primer. For cDNA synthesis, 1 μl of fluorophore-specific oligo(dT) primer was added to 8 μg of total RNA and the solution was incubated at 80°C for 10 min and then cooled on ice for 2 min. To each sample were added RNase inhibitor (Superase-In; Ambion) (1 μl), 5× first-strand buffer (4 μl), deoxynucleoside triphosphate (dNTP) mix (10 mM each dATP, dCTP, dGTP, and dTTP) (1 μl), 0.1 M dithiothreitol (DTT) (2 μl), and Superscript II RNase H^- reverse transcriptase (1 μl). Reverse transcription was carried out at 42°C for 2 h. The reaction was terminated by adding 0.5 M NaOH–50 mM EDTA (3.5 μl) and incubation at 65°C for 15 min and then neutralized with 1 M Tris-HCl (pH 7.5) (5 μl). For RNA expression-level comparison, samples were paired and concentrated using Microcon YM30 microconcentrators (Millipore) according to the manufacturer's protocol. Each sample pair (~20 μl) was suspended in formamide-based hybridization buffer (vial 7; Genisphere) (26 μl), Array 50dT blocker (Genisphere) (2 μl), and RNase/DNase-free water (4 μl). Two hybridizations were carried out in a sequential manner. The primary hybridization was performed by adding 48 μl of sample to the microarray under a supported glass coverslip (Erie Scientific) at 43°C for 16 to 20 h at high humidity. Prior to the secondary hybridization, slides were gently submerged into 2× SSC (1× SSC is 0.15 M NaCl plus 0.015 M sodium citrate)–0.2% SDS (at 43°C) for 11 min, transferred to 2× SSC (at room temperature) for 11 min, transferred to 0.2× SSC (at room temperature) for 11 min, and then spun dry by centrifugation. Secondary hybridization was carried out using the complementary capture reagents provided in the 3DNA Array 350 kit (Genisphere). For each reaction, the following were added: 3DNA capture reagent with Cy3 (2.5 μl), 3DNA capture reagent with Cy5 (2.5 μl), SDS-based hybridization buffer (vial 6; Genisphere) (26 μl), and RNase/DNase-free water (21 μl). The secondary hybridization solution was incubated in the dark at 80°C for 10 min followed by 50°C for 15 min. Hybridization was performed by adding 48 μl secondary hybridization solution to the slide under a supported glass coverslip at 65°C for 3 h at high humidity in the dark. At hybridization termination, arrays were gently submerged into 2× SSC–0.2% SDS (at 65°C) for 11 min, transferred to 2× SSC (at room temperature) for 11 min, transferred to 0.2× SSC (at room temperature) for 11 min, and then spun dry by centrifugation. To prevent fluorophore degradation, the arrays were treated with Dyesaver (Genisphere). For data analysis, slides were scanned on an Axon 4000B scanner (Molecular Devices) to detect Cy3 and Cy5 fluorescence. Laser

power was kept constant for Cy3/Cy5 scans, and the photomultiplier tube (PMT) setting was varied for each experiment based on optimal signal intensity with the lowest possible background fluorescence. A low-PMT-setting scan was also performed to recover signals from saturated elements. Gridding and analysis of images were performed using Genepix v6.1 (Molecular Devices). After background subtraction, median values were imported into the Partek genomics statistical analysis software. Values were $\log_2$ transformed, normalized by quantile, and readings lower than 10 were corrected to 10. For fold change and statistical validation of differences, we used two-way ANOVA, taking into account treatment and batch effects. Genes were considered differentially expressed if they presented a fold change equal to or higher than 2 and a *P* value of ≤0.05.

qRT-PCR. To validate the microarray data generated by the methodology, quantitative real-time PCR (qRT-PCR) was performed using the same RNA samples used for microarray experiments. For first-strand cDNA synthesis, equal amounts of total RNA (1 μg) were reverse transcribed (Superscript II; Invitrogen) using oligo$(dT)_{12–18}$ as primer. This cDNA was then used as the template in a qRT-PCR using SYBR green PCR reagents (Applied Biosystems) according to the manufacturer's recommendations. The amplification assays were performed on the ABI PRISM 7900HT sequence detection system (Applied Biosystems) in 8-μl reaction mixtures containing 0.5 μl of each primer (10 μM each), 4 μl of SYBR green PCR reagents (2×) (Applied Biosystems), and 0.2 μl of cDNA. After initial denaturation at 95°C for 10 min, amplifications were performed for 40 cycles at 95°C for 15 s, 58°C for 15 s, and 72°C for 20 s. To confirm the specificity of amplification, melting curves of PCR products were analyzed. The method applied in the analysis of the data from qRT-PCR was the threshold cycle (C_T) method, described by Livak and Schmittgen (17). The results were normalized to the expression of the housekeeping gene *ACT1*, which encodes the protein actin from *C. neoformans*. The experiment was performed in triplicate for all genes analyzed. All primers used are listed in Table 1.

Generation of ptp1Δ mutant strain. Targeted deletion of the *PTP1* gene was accomplished following the double-joint PCR strategy of Kim et al. (18). Briefly, we used PCR to fuse 5′- and 3′-flanking regions of the *PTP1* ORF to overlapping, incomplete segments of an expression cassette for the hygromycin phosphotransferase (*HYG*) gene under the control of the *C. neoformans* β-actin gene promoter. The two amplicons obtained were then simultaneously transformed in equimolar quantities into the *C. neoformans* KN99α strain following the biolistics procedure outlined by Toffaletti et al. (19). Transformants were picked under selection by hygromycin and the deletion of *PTP1* by homologous recombination with the two amplicons was confirmed by PCR. Southern blotting was used to confirm that a sole insertion event in the targeted locus had occurred. A qRT-PCR was also performed to confirm that the ptp1Δ mutant strain did not express the gene. Reconstitution of the native locus was achieved by simultaneous biolistic transformation of the mutants with an amplicon of the whole wild-type locus plus flanking regions and the plasmid pJAF1 containing the G418 (*NEO*) resistance cassette. $G418^+$ strains in which the HYG cassette had been expelled by the recombination event that restored *PTP1* were selected by their inability to grow on hygromycin.

Phenotype microarray. Phenotype microarray experiments (Biolog, Hayward, CA) were done as described previously by Nielsen et al. (20). Briefly, after overnight growth in YPD liquid medium, cells were collected by centrifugation, washed with sterile distilled H_2O, and resuspended at 10^5 cells/ml in 12% yeast nitrogen base liquid medium supplemented with histidine, leucine, and uracil. IFY-0 supplemented with 5 mg/ml ammonium sulfate, 0.85 mg/ml potassium phosphate monobasic, 0.15 mg/ml potassium phosphate dibasic, and 0.5 mg/ml magnesium sulfate was the inoculating fluid for the PM1 and PM2 phenotype microarray plates used (http://www.biolog.com/pdf/pm_lit/PM1-PM10.pdf). Cells were combined with supplemented IFY-0 at a ratio of 1:11, and 100 μl of this mixture was added to each well. All phenotype microarrays were incubated at 30°C, and the growth rate of each strain was checked by measuring the change in optical density at 492 nm (OD_{492}) over the course of 72 h. The phenotype microarray results were confirmed by growing the *C. neoformans* KN99α, ptp1Δ, and ptp1Δ::ptp1 strains in minimal medium (10 mM $MgSO_4$, 29.3 mM KH_2PO_4, 13 mM glycine, 3 mM thiamine [pH 5.5]) with 1% glucose or mannitol as the only carbon source. *C. neoformans* D1307 mutant and H99 wild-type strains were compared for the growth rate in minimal medium with 1% of the chosen carbon source, 10 mM $MgSO_4$, 29.3 mM KH_2PO_4, 13 mM glycine, and 3 mM thiamine (pH 5.5). The sole carbon sources used were glucose, mannose, galactose, xylose, mannitol, sorbitol, dulcitol, ribitol, arabitol, and maltitol. Cultures were incubated for 48 h at 30°C, and growth was checked by measuring the change in optical density at 630 nm every 12 h.

TABLE 1 Primers for *C. neoformans* genes used in real-time PCR experiments

Primer	Gene product	Sequence (5′→3′)
Act F	Actin	TTGTCCTCCCCAATCTTCAC
Act R		CGGCGACTTCTTCTTCCATA
Ptp1 F	Polyol transporter protein 1	TACCGTCCCCATCTTCTCTG
Ptp1 R		ATACCAGCAACGACCCAAAG
Cat3 F	Catalase 3	GTTAAACCAAGCCGCCAATA
Cat3 R		CTGATACCTTGACCCCGAAA
Ths F	Trehalose synthase	GCCCAAAGAAGTGGAGATCA
Ths R		AGAGCTCCATTGCTCCAGAA
Plc F	Phospholipase C	GTCTTTGTCATGGGCGACTT
Plc R		TAGCCGAAGGATGAACTTGG
Gbe F	1,4-α-Glucan-branching enzyme	ATCCTTGGCTGGAACCTTTT
Gbe R		CTTTGAGAATTCGGCGAGAC
Aox F	Alternative oxidase	CCCATTTACACCGAGAAGGA
Aox R		AGGAACTTGACGGTCCTGTG
Erg3 F	C-5 sterol desaturase	CCCAGTCCCTTCCTTACCAT
Erg3 R		TCATATCACCGTCGTGGATG
Erg11 F	Lanosterol 14 α-demethylase	TCCCATCCACTCGATCTACC
Erg11 R		CCCTTGGGGATGATGTATTG
Mls F	Malate synthase	AAACATGGTTCTCGGACAGG
Mls R		AGGTCGAACCAAAAGCACAG

Evaluation of virulence factors expression *in vitro*. We used 24-h exponential-phase cultures of the fungus growing in liquid YPD at 30°C under moderate (100-rpm) rotation. Resistance to different stressing agents was tested by serial, five-step 10-fold dilutions of the fungus, starting from 5×10^4 cells per agar spot. To evaluate thermoresistance, the growth rates of wild-type and mutant strains at 37°C were compared as follows. To test for resistance to cell wall-destabilizing agents, the fungus was grown on solid YPD containing Congo red (1% [mass/vol]) or calcofluor white (250 μg/ml) at 37°C or SDS (0.1% [mass/vol]) at 30°C. For resistance to salt stress, the fungus was grown on 1.5 M NaCl in solid YPD at 30°C. The ability to produce phospholipase and urease was tested by spotting 10-μl suspensions containing 10^3 cells onto solid YPD containing 8% (vol/vol) egg yolk (21) and Christensen's urea agar (0.1% peptone, 0.5% NaCl, 0.2% KH_2PO_4, 0.1% glucose, 2% urea, 0.0016% phenol red), respectively. To evaluate melanin production, *C. neoformans* strains were grown in chemically defined minimal medium (15 mM dextrose, 10 mM $MgSO_4$, 29.4 mM KH_2PO_4, 13 mM glycine, 3 μM thiamine [pH 5.5]) with 1 mM L-DOPA (L-3,4-dihydroxyphenylalanine) (Sigma-Aldrich) and incubated at 30°C in the dark.

Capsule size measurements. *C. neoformans* wild-type and mutant strains were grown for 24 h in YPD medium at 30°C, collected by centrifugation, washed twice with 1× PBS, and cultured for 48 h in minimal medium (10 mM $MgSO_4$, 29.3 mM KH_2PO_4, 13 mM glycine, 3 mM thiamine [pH 5.5]) with 1% glucose or mannitol as only carbon source. Cultures of *C. neoformans* were diluted in 1× PBS, and an aliquot of each sample was mixed with a drop of India ink (BD Biosciences, NJ). Inspection was performed in an Axiovert 200 M inverted microscope (Carl Zeiss Micro Imaging, NY). Capsule size was measured with the ImageJ 1.39g software (National Institutes of Health, Bethesda, MD) as the distance between the capsule border and the cell wall, corresponding to the India ink exclusion zone. The size of the cell body was also measured. At least 150 yeast cells were evaluated for each experimental condition.

Measurement of mannitol secretion by *C. neoformans* cells. *C. neoformans* cells were inoculated in YPD medium and grown overnight at 30°C. On the following day, the cells were washed 3 times and inoculated at 1.8×10^8 cells/ml in 10 mM potassium phosphate buffer containing glucose at 100 mM and incubated at 30°C with agitation for 3 h, as described before (22). Samples were collected at 0, 1, and 3 h, centrifuged, filtered through a 0.2-μm membrane to remove cells, and analyzed for mannitol in a Shimadzu high-performance liquid chromatography (HPLC) system (Kyoto, Japan) equipped with a refractive index detector. The analysis was performed in isocratic mode at 85°C using a Bio-Rad Aminex HPX-87P column and Milli-Q water as the mobile phase at a flow rate of 0.6 ml/min. A 4-level calibration standard curve was created for commercial glucose and mannitol. The amounts of mannitol and glucose in each sample were calculated using the LCsolution software (Shimadzu, Kyoto, Japan).

Mouse virulence studies. Groups of 6- to 8-week-old female BALB/c mice (10 mice per group) were obtained from the National Cancer Institute. Intratracheal infection was performed as previously described by Feldmesser and Casadevall (23). Briefly, strains of *C. neoformans* were cultured in YPD liquid medium (24 h, 30°C, 150 rpm), collected by centrifugation (1,800 × *g* for 10 min), washed, and resuspended in 1× PBS to a final cell concentration of 2×10^7 cells/ml. Mice were intraperitoneally anesthetized with 100 mg/kg ketamine and 10 mg/kg xylazine. Fifty microliters of the fungal suspension was slowly injected into the previously exposed trachea. The number of live mice was monitored daily. The experiment was repeated twice. The data presented here are from a representative experiment. All animal experiments were previously approved by the Institutional Animal Care and Use Committee of Albert Einstein College of Medicine.

Quantitative analysis of tissue fungal burden. Groups of 4- to 6-week-old female BALB/c mice (five mice per strain) infected intratracheally with *C. neoformans* strains were sacrificed by CO_2 inhalation at 10 days postinfection. The lungs and brains were removed, weighed, and homogenized in 5 ml sterile 1× PBS. Serial dilutions of the organ samples were plated on Sabouraud agar plates and incubated at 30°C for 48 h. Colony counts were performed and adjusted to reflect the total number of CFU/g tissue.

***Galleria mellonella* survival experiments.** *Galleria mellonella* infection was performed as previously described by Garciá-Rodas et al. (24). Briefly, *G. mellonella* larvae (Vanderhorst Wholesale, Inc., St. Marys, OH, and Mous Livebait R.J., The Netherlands) were inoculated with 10 μl of a 10^6-cell/ml yeast suspension by an injection in the last left pro-leg using a sterile 26-gauge needle-fitted Hamilton syringe. Infected larvae were incubated at 25 or 37°C, and the number of dead caterpillars was scored daily. A group of *G. mellonella* larvae was inoculated with 1× PBS as a control for physical injury; another group without any manipulation was set as an untreated control. This experiment was repeated twice. The data presented here are from a representative experiment.

Statistical analyses. GraphPad Prism 5.0 (GraphPad Software) was used for statistical analyses. The paired two-tailed Student's *t* test was performed for phenotype microarray, capsule size measurement, and CFU experiments. The log rank test was performed to evaluate statistical differences on survival curves. A *P* value of ≤0.05 was considered significant.

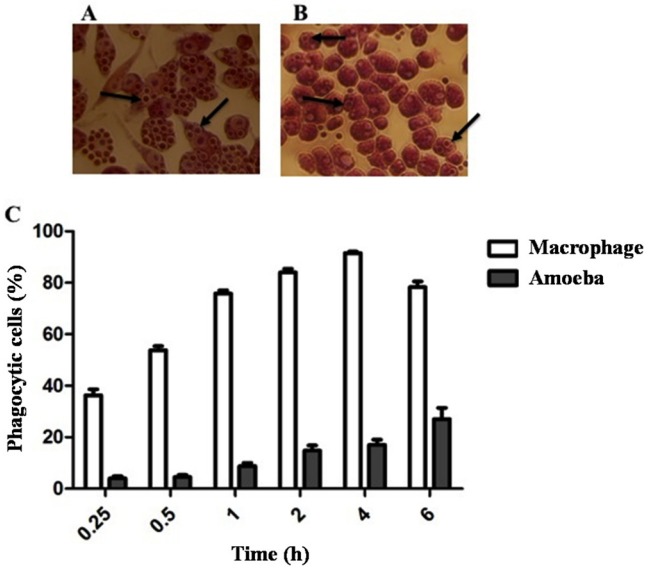

FIG 1 Kinetics of *C. neoformans* phgocytosis by amoeba and murine macrophages over 6 h. Yeast cells were incubated with amoebae (28°C) or macrophages (37°C and 5% CO_2 atmosphere) in a ratio of five *C. neoformans* yeast cells per host cell. Microphotographs (×40) representing results 6 h postinfection of macrophages (A) and amoebae (B) with *C. neoformans* are shown above the histogram. The arrows show internalized fungal yeast cells. (C) Percentages of macrophages (white bars) and amoebae (gray bars) containing internalized *C. neoformans*. These experiments were performed in quadruplicate (mean ± standard error of the mean [SEM]).

Microarray data accession number. The microarray data generated by this study have been deposited into the Gene Expression Omnibus (GEO) (http://www.ncbi.nlm.nih.gov/geo/) under accession no. GSE45027.

RESULTS

Kinetics of *C. neoformans* phagocytosis by amoebae and murine macrophages. We carried out an analysis of the kinetics of *C. neoformans* internalization by the amoeba *A. castellanii* and murine macrophages to ascertain the optimal time intervals for carrying out experiments. After 4 h of coculture with macrophages, more than 90% contained yeast cells (Fig. 1C). This percentage decreased after 6 h, possibly due to exocytosis of the fungus, which can occur with or without lysis of the host cell (25, 26). The percentage of phagocytosis of *C. neoformans* by amoebae, however, increased progressively throughout the period evaluated. After 6 h, about 30% of amoebae contained yeasts (Fig. 1C). Encapsulated *C. neoformans* cells are known to resist ingestion by amoeba (27), and given the low efficiency of phagocytosis by *A. castellanii in vitro*, 6 h was chosen as the time point for gene expression profiling of *C. neoformans* recovered from phagocytic cells. Figures 1A and B are representative photomicrographs of macrophages and amoebae, respectively, after 6 h of infection with *C. neoformans*.

Transcriptional profile of *C. neoformans* inside amoebae and macrophages. The microarray was used to compare the transcriptional profiles of *C. neoformans* cells upon interaction with *A. castellanii* and murine macrophages. Total RNA was extracted from fungal cells either internalized by phagocytes or grown in the corresponding culture medium (control) for 6 h. All RNA prepa-

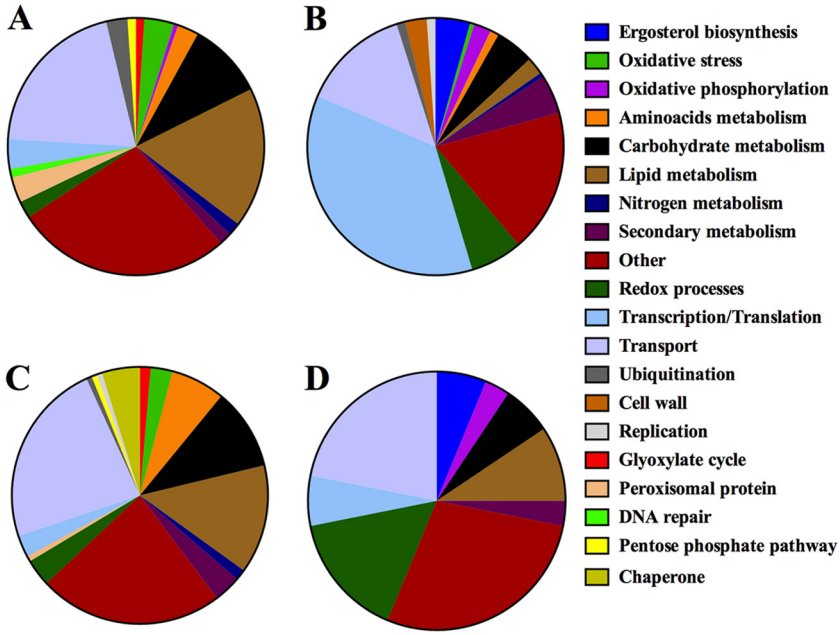

FIG 2 Classification of *C. neoformans* genes modulated after intracellular residence in *A. castellanii* and murine macrophages. *C. neoformans* genes induced (A) or repressed (B) after internalization by *A. castellanii*. *C. neoformans* genes induced (C) or repressed (D) after internalization by murine macrophages.

rations satisfied the criteria of integrity, and no contamination with host cell RNA was detected (data not shown).

Analysis of the differential gene expression of *C. neoformans* during *A. castellanii* infection indicated modulation of 656 genes from a total of 7,775 genes represented in the microarray assay. (For a complete list, see the supplemental material.) Of these, 322 genes were upregulated more than 2-fold, including genes encoding proteins related to nutrient transport, general metabolism, and oxidative stress response (Fig. 2A), while 334 genes were downregulated (Fig. 2B). Among the latter were genes encoding proteins involved in transcription, translation, and ergosterol biosynthesis. Additionally, genes encoding well-established *C. neoformans* virulence factors for mammalian hosts were also modulated during amoeba infection.

A similar analysis was performed to evaluate the transcriptional profile of *C. neoformans* interacting with murine macrophages for 6 h. The results showed a total of 293 genes whose expression was modulated more than 2-fold in response to the macrophage microenvironment (for a complete list see the supplemental material). The 222 genes of *C. neoformans* with increased expression included those encoding transporters, chaperones, and proteins involved in the oxidative stress response and metabolism (Fig. 2C). Genes related to ergosterol biosynthesis and oxidative phosphorylation were suppressed, as shown in Fig. 2D.

To validate the data obtained by the microarray assay, qRT-PCR analysis was performed for some *C. neoformans* genes previously identified in our microarray studies to be modulated in response to the phagocytes' intracellular niches. To correct for differences in RNA quantity among the samples, the gene encoding the actin protein was used as a control. The expression profiles for all genes analyzed by qRT-PCR matched the microarray results with respect to direction (up or down) of modulation (Fig. 3).

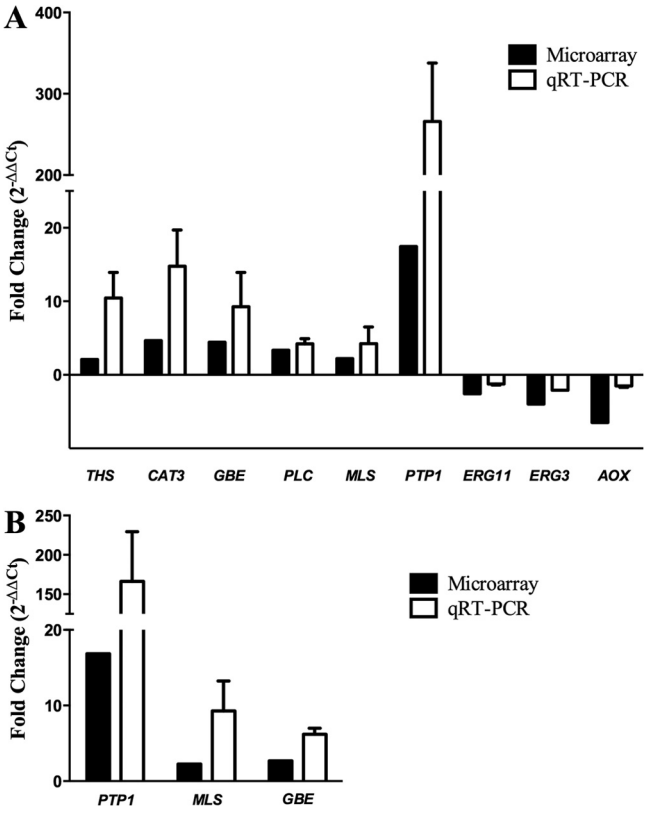

FIG 3 Validation of microarray data by real-time PCR. *C. neoformans* gene expression after 6 h interaction with *A. castellanii* (A) and murine macrophages (B). The products of the genes shown are as follows: *THS*, trehalose synthase; *CAT3*, catalase 3; *GBE*, 1,4-α-glucan branching enzyme; *PLC*, phosphoryl inositol sphingolipid phospholipase C; *MLS*, malate synthase; *PTP1*, polyol transporter protein 1; *ERG11*, lanosterol 14 α-demethylase; *ERG3*, C-5 sterol desaturase; and *AOX*, alternative oxidase.

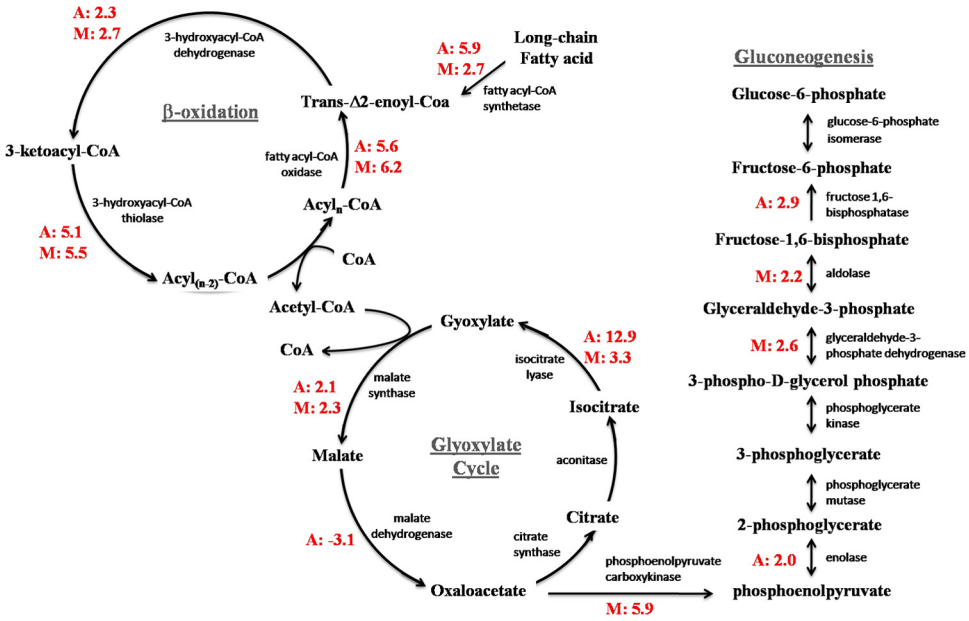

FIG 4 *C. neoformans* reprogramming of carbon metabolism in response to phagocytosis by amoeba and macrophages. The metabolic pathway scheme shows the differential modulation of several transcripts of enzymes active in gluconeogenesis, glyoxylate cycle, and β-oxidation after *C. neoformans* internalization by amoebae (A) and macrophages (M).

A comparative analysis of transcriptional changes in amoebae and macrophages showed that 111 genes were similarly modulated in response to both intracellular environments. This represents 38% of all genes differentially expressed by *C. neoformans* during macrophage interaction. Of these genes, 63.1% were induced, while 20.7% were repressed in both intracellular niches. Among the genes whose expression was increased in both macrophages and amoebae, those involved in nutrient transport, oxidative stress response, and general metabolism stand out. In fact, the metabolic responses of *C. neoformans* to interaction with macrophages and amoebae were very similar. Overall, our results indicate a metabolic switch from glycolysis to gluconeogenesis and fatty acid degradation for conversion to glucose via the glyoxylate cycle (Fig. 4). Conversely, genes related to ergosterol biosynthesis were suppressed after internalization of *C. neoformans* by both phagocytic cells (Table 2).

Although the majority of yeast genes (83.8%) commonly expressed during interaction with both phagocytes were similarly modulated, suggesting that the intracellular environments of amoeba and macrophages are quite comparable, 16.2% of the identified genes were differently modulated (Table 3). Most of them encode hypothetical proteins (39%), transporters (22.2%), and proteins related to metabolism (11.1%), suggesting differences in nutrient availability within phagosomes of macrophages and amoebae.

Functional study of the *C. neoformans* ORF CNAG_05662. The comparison of *C. neoformans* transcriptomes upon internalization by amoebae and macrophages allowed the identification of genes potentially related to its survival inside host cells. The presumed importance of those genes in *C. neoformans* adaptation to the harsh phagosome environment translates into a potential role in virulence. Based on the expression levels of *C. neoformans* genes during interaction with host cells, some were selected for future assessment of their relevance in the establishment of cryptococcosis. Among them, the ORF CNAG_05662, which codes for a sugar transport motif (http://motif.genome.jp/) of 631 amino acids, was particularly interesting since it was strongly induced, by 17.4- and 16.8-fold in amoebae and macrophages, respectively (Table 2). Additionally, the quantitative analysis by qRT-PCR revealed induction levels on the order of 250- and 150-fold upon internalization by amoebae and macrophages, respectively (Fig. 3).

To characterize the function of the ORF CNAG_05662 and investigate its role in the virulence of the fungus, both a strain in which this gene has been mutated (ptp1Δ) and a strain in which this gene has been complemented (ptp1Δ::ptp1) were generated. Southern blotting was performed to confirm a sole insertion event in the targeted locus, and qRT-PCR was performed to confirm that the mutant strain did not express the CNAG_05662 gene, while the complemented strain did (data not shown).

Since the predicted function for the product of CNAG_05662 was related to sugar transport, a phenotype microarray was performed to compare the growth of wild-type (WT), mutant (Mut), and complemented (Rec) strains after 72 h of culture in various carbon sources. Using the PM1 and -2 assays (Biolog, Hayward, CA), we observed that the mutant strain was not able to grow when the carbon source was in the form of polyols, such as D-mannitol, D-sorbitol, dulcitol, arabitol, and adonitol (Fig. 5). This suggested that CNAG_05662 coded for a protein related to the transport of 5- and 6-carbon polyols. In contrast, the fungus was able to grown when erythritol and maltitol were used as carbon sources, suggesting that this gene is not involved in the transport of molecules of 4 and 12 carbons, respectively (Fig. 5). The microarray phenotype was validated assessing the growth curve of the wild-type (WT), mutant (Mut), and complemented (Rec) strains using glucose or mannitol as the carbon source (see Fig. S1 in the supplemental material). Alternatively, we compared the results for the mutant constructed in this work with those for a strain (D1307) obtained from a mutant library constructed by Liu et al.

TABLE 2 *C. neoformans* genes with similar modulation patterns after interaction of the fungus with amoebae and murine macrophages

Category	Accession no.[a]	Predicted function	Fold change in:	
			Amoebae	Macrophages
Ergosterol biosynthesis	CNAG_04687	Stearoyl-CoA 9-desaturase	−2.82949	−2.5887
	CNAG_01737	C-4 methyl sterol oxidase	−5.10666	−2.1578
Oxidative phosphorylation	CNAG_05626	h-sco1	−3.39215	−2.02884
Glyoxylate cycle	CNAG_05303	Isocitrate lyase	3.32005	12.9474
	CNAG_05653	Malate synthase	2.09609	2.26303
Oxidative stress	CNAG_02147	Cytochrome *c* peroxidase	3.59838	5.1284
	CNAG_01846	Flavoprotein	3.11961	2.0610
	CNAG_05169	Cytochrome b_2	2.68905	2.7162
Transcription	CNAG_04345	RNA polymerase II transcription factor	2.59053	2.40314
Transport	CNAG_07869	Sugar transporter	24.5501	5.20518
	CNAG_05662	Sugar transporter	17.4444	16.8462
	CNAG_01384	bodown198	8.88579	4.86666
	CNAG_01936	Sugar transporter	6.84072	7.29332
	CNAG_03772	Glucose transporter	6.70411	11.1359
	CNAG_03910	D-Xylose-proton symporter	6.64142	2.84406
	CNAG_03060	Multidrug resistance protein	6.03422	2.11251
	CNAG_01925	Conserved hypothetical protein	4.10947	2.45472
	CNAG_05685	Neutral amino acid transporter	3.44863	2.77709
	CNAG_05929	MFS maltose permease MalP	2.95817	3.30233
	CNAG_02288	Succinate:fumarate antiporter	2.68543	4.94611
	CNAG_07367	Amino acid transporter	2.42433	3.12233
	CNAG_04795	Adenine nucleotide transporter	2.26578	2.83099
	CNAG_07387	Siderophore-iron transporter Str3	−2.04064	−2.56502
	CNAG_03438	Hexose transporter	−3.94741	−2.56777
Pentose phosphate pathway	CNAG_00827	Ribose 5-phosphate isomerase	3.00641	7.41447
Amino acid metabolism	CNAG_03128	Lincomycin-condensing protein lmbA	2.27524	2.19625
Carbohydrate metabolism	CNAG_04621	Glycogen synthase	5.22439	2.17416
	CNAG_03067	Pyruvate carboxyltransferase	3.79568	2.66549
	CNAG_00393	1.4-α-Glucan-branching enzyme	3.33816	2.70596
	CNAG_04659	Pyruvate decarboxylase	−3.97919	−2.58975
Lipid metabolism	CNAG_03019	Long-chain-fatty-acid-CoA ligase	5.87013	2.70475
	CNAG_06431	Acyl-CoA oxidase	5.64239	6.20667
	CNAG_00490	Acetyl-CoA C-acyltransferase	5.09895	5.5079
	CNAG_03666	Acyl-CoA dehydrogenase	5.08676	5.62055
	CNAG_06551	Carnitine O-acetyltransferase	4.5781	5.56428
	CNAG_07747	Acyl-CoA oxidase I	4.54934	2.41408
	CNAG_02562	Acyl-CoA dehydrogenase	4.19328	2.79301
	CNAG_02045	Acetoacyl-CoA synthetase	3.65055	2.95075
	CNAG_03393	Acyl-CoA thiolesterase	3.56595	2.11571
	CNAG_05721	Peroxisomal hydratase-dehydrogenase-epimerase	3.16504	3.29229
	CNAG_01116	β-Ketoacyl reductase	3.06954	2.80628
	CNAG_04392	Sterol-binding protein	2.83953	3.82553
	CNAG_00537	Carnitine acetyltransferase	2.7752	3.02984
	CNAG_04238	2.4-Dienoyl-CoA reductase	2.71898	2.7285
	CNAG_00371	Enoyl-CoA hydratase	2.34604	3.14993
	CNAG_04308	Short-chain 3-hydroxyacyl-CoA dehydrogenase	2.32894	2.66174
	CNAG_01671	Acetyl/propionyl CoA carboxylase	2.12004	3.93367
	CNAG_00499	Carnitine/acyl carnitine carrier	2.10977	3.88855
	CNAG_06628	Aldehyde dehydrogenase	2.74167	6.49193
	CNAG_02087	Sphingosine *N*-acyltransferase	−7.58831	−3.75872

(Continued on following page)

TABLE 2 (Continued)

Category	Accession no.[a]	Predicted function	Fold change in: Amoebae	Fold change in: Macrophages
Nitrogen metabolism	CNAG_03243	2-Nitropropane dioxygenase	3.40319	3.0279
	CNAG_05644	2-Nitropropane dioxygenase	2.16675	4.29356
Secondary metabolism	CNAG_06623	*myo*-Inositol oxygenase	2.52692	2.13304
Redox processes	CNAG_05299	Oxidoreductase	3.16418	3.35935
	CNAG_00541	Dimethylaniline monooxygenase	−3.47134	−2.62673
	CNAG_01939	fmHP	−5.14025	−2.08856
	CNAG_02577	Oxidoreductase	−5.33935	−2.63942
Other	CNAG_01702	Integral membrane protein	11.4333	3.68741
	CNAG_05229	Stomatin family protein	5.47933	2.29192
	CNAG_02295	Phosphotransferase enzyme family domain-containing protein	4.64925	2.60426
	CNAG_07862	Fumarate reductase	3.94316	9.98097
	CNAG_01252	Thiosulfate sulfurtransferase	3.08677	2.65488
	CNAG_01794	2-Hydroxyacid dehydrogenase	2.68166	2.99315
	CNAG_04096	Racemase	2.09515	2.30145
	CNAG_02674	dJ347H13.4	2.05302	2.52509
	CNAG_04103	DUF895 domain membrane protein	2.02542	2.75068
	CNAG_02264	AFG1-family ATPase	−2.25762	−2.26571
	CNAG_05370	Integral membrane protein	−4.69223	−2.34957
Hypothetical protein	CNAG_04837		7.15172	6.35904
	CNAG_03394		4.22103	2.59575
	CNAG_02405		3.51154	3.46188
	CNAG_02978		3.17452	3.07828
	CNAG_01847		3.06055	2.00546
	CNAG_06583		2.76876	2.92177
	CNAG_04394		2.75153	2.64509
	CNAG_00079		2.74434	2.5312
	CNAG_05784		2.67849	2.69336
	CNAG_06355		2.65531	2.26161
	CNAG_02044		2.3962	4.54104
	CNAG_07708		2.33125	2.78776
	CNAG_07912		2.01817	3.91411
	CNAG_00315		2.00838	2.82288
	CNAG_03857		−2.04111	−2.09241
	CNAG_00349		−2.05716	−2.90138
	CNAG_07568		−2.19254	−2.23732
	CNAG_02910		−2.45926	−2.39798
	CNAG_00814		−4.9423	−2.36478
	CNAG_07920		−5.37886	−3.4471
	CNAG_04891		−5.38601	−2.13027
	CNAG_01803		−5.56394	−2.8793
	CNAG_05741		−5.82377	−2.40385
	CNAG_01369		−8.89767	−2.03519
	CNAG_06590		−11.3003	−3.06825

[a] Accession numbers of genes listed in the homepage of the *Cryptococcus neoformans* var. *grubii* genome assembled by the Broad Institute of MIT and Harvard (http://www.broadinstitute.org/annotation/genome/cryptococcus_neoformans).

(16) in which the same ORF was deleted. The lack of expression of the gene in the D1307 mutant strain was confirmed by qRT-PCR (data not shown). Incubation of the D1307 strain in different carbon sources for 48 h revealed no growth when mannitol, sorbitol, dulcitol, ribitol, and arabitol were used as the sole carbon sources (see Fig. S2 in the supplemental material), confirming the function of the gene. Consequently, we have named the product of CNAG_05662 "polyol transporter protein 1" (Ptp1).

Next we assessed whether Ptp1 function was related to mannitol transport out of the cell by inducing and quantifying its secretion by the wild-type, mutant, and reconstituted strains *in vitro*. Our results showed no statistically significant difference in mannitol secretion levels among them (data not shown), suggesting that Ptp1 is only involved in the transport of polyols into the cell.

Role of the *PTP1* gene in the virulence of *C. neoformans*. To assess whether expression of *PTP1* is related to virulence in *C. neoformans*, we evaluated the ability of the mutant strain to express known virulence factors *in vitro*. Our results showed no differences in several phenotypes implicated in virulence, such as growth at 37°C, melanin production, and urease and phospho-

TABLE 3 *C. neoformans* genes with different modulation patterns after interaction of the fungus with amoeba and murine macrophages

Category	Accession no.[a]	Predicted function	Fold change in:	
			Amoebae	Macrophages
Amino acid metabolism	CNAG_05676	Tyrosine aminotransferase	−3.30706	3.31586
Lipid metabolism	CNAG_00984	Glucose and ribitol dehydrogenase protein	3.2289	−2.10481
Redox processes	CNAG_04085	Oxidoreductase	−4.76438	3.27837
	CNAG_00876	Ferric-chelate reductase	−2.39397	2.68318
Translation	CNAG_03563	Aspartate-tRNA ligase	2.02203	−2.59223
Transport	CNAG_04758	Ammonium transporter	2.41737	−2.39166
	CNAG_04210	Sugar transporter	−2.3879	2.78891
	CNAG_03426	GDP-mannose transporter	−2.94678	3.16533
	CNAG_00895	Zinc ion transporter	−4.53653	2.67154
Other	CNAG_03759	Conidiation-specific protein 6	5.73768	−4.86503
	CNAG_06576	Allergen	2.38555	−2.92608
Hypothetical protein	CNAG_03068		9.56139	−2.24987
	CNAG_02694		4.11009	−2.25959
	CNAG_00848		3.1508	−2.19634
	CNAG_02362		2.74084	−2.04115
	CNAG_06396		2.15314	−2.57459
	CNAG_01865		−2.36364	4.66234
	CNAG_00813		−5.87379	4.67373

[a] Accession numbers of genes listed in the homepage of the *Cryptococcus neoformans* var. *grubii* genome assembled by the Broad Institute of MIT and Harvard (http://www.broadinstitute.org/annotation/genome/cryptococcus_neoformans).

lipase synthesis. The deletion of *PTP1* did not result in changes in capsule size when yeast cells were grown in glucose as the only carbon source. However, in contrast to the wild-type strain, the ptp1Δ mutant strain did not increase capsule size in response to mannitol (Fig. 6).

The role of Ptp1 in the virulence of *C. neoformans in vivo* was investigated comparing the pathogenic potentials of KN99α and ptp1Δ strains using mice and *G. mellonella* as infection models. The results suggest that these two strains are equivalent in their abilities to establish cryptococcosis in both standard models, since no difference in survival rates of mammalian and invertebrate hosts was observed (Fig. 7A to C). To confirm that KN99α and ptp1Δ strains cause disease in the same way, as suggested by the survival results, we checked the CFU numbers in the lungs and brains of mice at an intermediate time point in the infection (10 days). As shown in Fig. 7D and E, no differences were observed in lung and brain fungal burdens.

To assess the role of the *PTP1* gene *C. neoformans*, macrophages and amoebae were infected with both KN99α and ptp1Δ strains for 6 h, and the survival rate of internalized yeast cells was calculated by the number of fungal CFU obtained from lysed host cells. The results show that the ptp1Δ strain exhibited no significant difference in survival compared to the wild type (data not shown). Also, the abilities of macrophages and amoebae to ingest the KN99α and ptp1Δ strains were similar, as measured by the phagocytosis kinetic assay (data not shown).

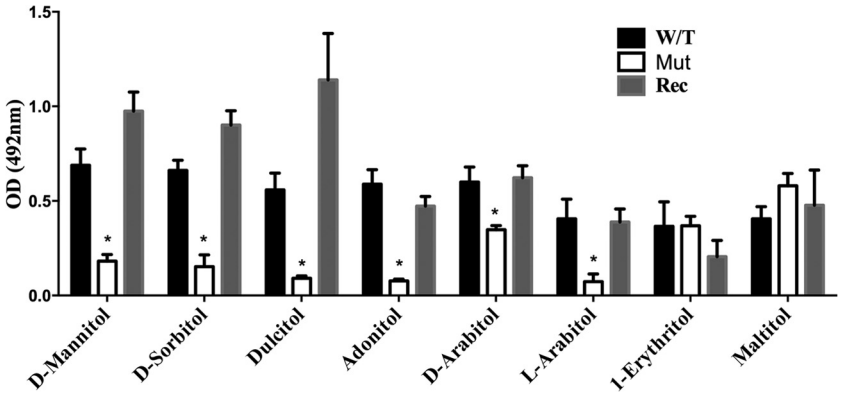

FIG 5 Growth rate of KN99α (wild type [W/T]), mutant (Mut), and complemented (Rec) strains of *C. neoformans* in media with different polyols as sole carbon sources. Yeast cells were cultivated at 30°C for 72 h, and the growth rate was verified by monitoring for color change in the wells and by measuring the variation of optical density at 492 nm as described for the phenotype microarray assay. The *t* test was performed using GraphPad Prism 5. *, $P < 0.05$.

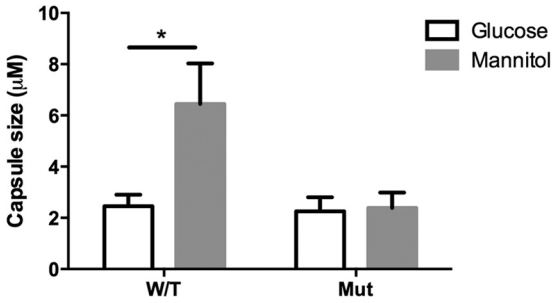

FIG 6 Capsule diameter of *C. neoformans* KN99α (wild-type [W/T]) and mutant (Mut) strains grown in glucose or mannitol as unique carbon sources. The capsule diameter was calculated as the difference between the whole-cell size and the cell body size. The capsule size of 150 yeast cells was measured for each condition. The *t* test was performed using GraphPad Prism 5. *, $P < 0.05$.

DISCUSSION

The capacity of the saprophytic fungus *C. neoformans* for mammalian pathogenesis has been suggested to arise by selection of traits that function in virulence through the interaction with soil predators (28), among which amoebae are of particular interest, since they share certain characteristics with mammalian phagocytic cells, such as macrophages. In fact, the amoebae have been shown to be predators of *C. neoformans* that influence its survival in soils (29, 30). Several studies have shown parallels in the interaction of *C. neoformans* with macrophages and amoebae (12, 27, 31). Although these reports support the environmental selection hypothesis, no study to date has focused on the molecular mechanisms central to the adaptation of *C. neoformans* to the intracellular environment of soil predators that may have allowed it to survive inside mammalian host cells.

If the amoeba hypothesis is correct, one might predict similar *C. neoformans* transcriptional profiles when it interacts with macrophages and protozoa. To test this prediction, we compared the transcriptional profiles of *C. neoformans* 6 h after phagocytosis by the amoeba *A. castellanii* and by murine macrophages. In planning our experimental design, we needed to take into account that the interactions between *C. neoformans* and amoeba and macrophages occur in very different environments. *C. neoformans*-amoeba interactions occur at ambient temperatures in soils, which are usually acidic. In contrast, *C. neoformans*-macrophage interactions occur at 37°C in near-neutral pHs. Thinking through our experimental options, we considered carrying out amoeba-cryptococcus interactions at higher temperatures and or macrophage-cryptococcus interactions at lower temperatures to harmonize the physical conditions but opted against such experiments because they would have represented a highly constrained comparison with little or no relevance to reality. Instead, we focused on comparing these interactions under conditions that approximated the natural interactions, fully aware that differences in temperature and media would introduce additional variables. However, by focusing only on the subset of gene responses induced or repressed by both amoeba and macrophage interactions relative to those outside, we avoided focusing on transcriptional differences resulting from different environmental conditions. We note that classic experiments such as those showing that bacteria use similar virulence genes for plants and animals also required infection of their hosts at different temperatures (32).

Our transcriptional analysis showed totals of 656 and 293 induced genes in *C. neoformans* ingested by amoebae and macrophages, respectively, whose expression was changed at least 2-fold relative to nonphagocytosed cells. These results allowed us to compare the adaptation of *C. neoformans* to the intracellular environment of the two hosts on a molecular level. It is interesting that the number of *C. neoformans* genes induced by the interaction with amoebae was more than two times greater than the number induced upon interaction with macrophages. Although the mechanism responsible for this difference is not understood, we note that an amoeba is a free-living organism that feeds by microbial predation and that it must encounter a very diverse microbiota in soils. Consequently, amoebae may have more versatile microbial killing and digesting mechanisms than macrophages, which would submit *C. neoformans* to greater stress, leading to a more extensive transcriptional response. Alternatively, the number of genes induced after the interaction with macrophages may be smaller than that observed with the amoeba because *C. neoformans*-macrophage experiments were carried out at 37°C and the higher temperature can itself induces stress on fungal cells. Despite these differences, the overall categorization of the protein-coding genes revealed a very similar gene expression profile of the fungus inside either phagocyte. We have analyzed the transcriptional response by focusing on gene functional categories.

Gene functional categories. (i) Genes related to the transport of ions and small molecules. Although little is known concerning the nutritional composition of the phagosome, it is assumed that this organelle is poor in carbon and amino acid sources (33, 34). This nutritional stress induces an adaptive response in intracellular pathogens to allow for survival within phagocytes (4, 9, 35, 36). For example, expression of genes encoding transporter proteins can be translated into more effective assimilation of available nutrients. In agreement with the notion that *C. neoformans* residence in the phagosome translates into a starvation state, our results show that about 10% of the genes modulated after internalization by amoebae and 13.7% of those genes modulated in response to the macrophage are related to nutrient transport. Fan et al. (4) also reported the transcriptional induction of various *C. neoformans* transporters after 2 and 24 h of cocultivation with activated macrophages. In addition, Hu et al. (37) identified a large amount of transporters potentially important for the growth of *C. neoformans* in the lungs of infected mice.

One of the most highly differentially expressed genes by *C. neoformans* in macrophages and amoebae was the ORF CNAG_05662, which was deduced to be a sugar transporter based on amino acid homology to known proteins. Functional experiments determined that this gene encoded a protein related to the transport of 5- and 6-carbon polyols, which was named Ptp1 (polyol transporter protein 1). The evidence that the *PTP1* gene product is involved with mannitol transport was particularly interesting since some studies have correlated the secretion of this polyol by *C. neoformans* with progression of pathogenesis. The production of D-mannitol by *C. neoformans* occurs both *in vitro* (38) and *in vivo* and contributes to the pathogenesis of meningoencephalitis (39) and virulence in mice (40). Ptp1 appeared to have a role only in the transport of mannitol into the fungal cell and was not involved in its secretion by *C. neoformans*. Disruption of the *PTP1* gene had no effect on the expression of virulence factors by *C. neoformans in vitro*, such as melanin, urease, and phospholipase. The capsule size of the mutant strain was only affected during growth in mannitol as the sole carbon source.

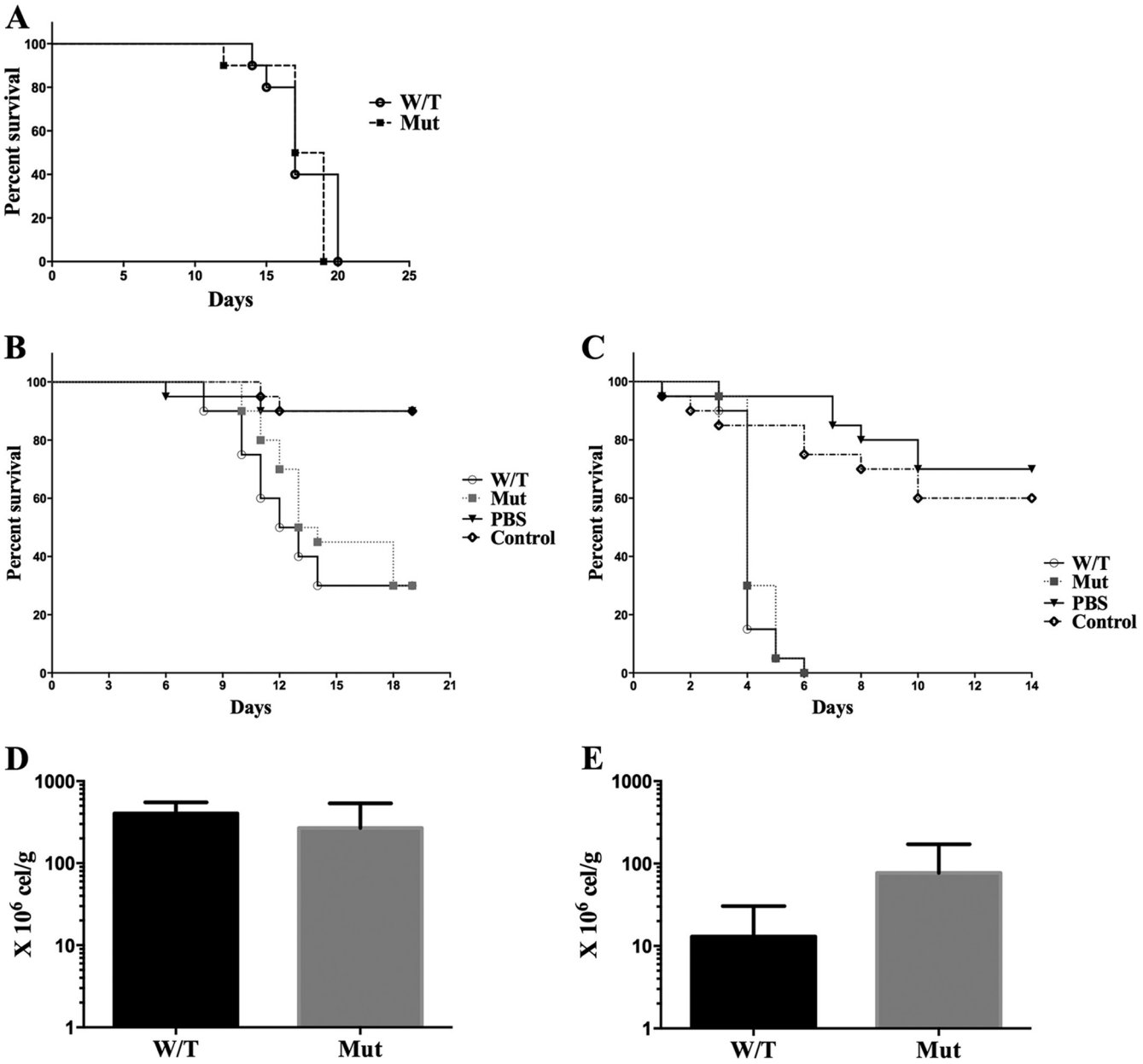

FIG 7 Assessment of *in vivo* virulence of the ptp1Δ mutant strain. (A) Survival curve of mice infected with KN99α (wild-type [W/T]) and mutant (Mut) strains of *C. neoformans*. BALB/c mice (10 per group) were intratracheally infected with 10^6 yeast cells, and mortality was monitored daily. No statistical difference was found by comparing the curves for wild-type and mutant strains. (B and C) Survival curves of *Galleria mellonella* infected with the KN99α (W/T) and mutant (Mut) strains of *C. neoformans*. Larvae were infected with 10^4 yeast cells and maintained at 25°C (A) or 37°C (B). (D and E) Tissue burden of *C. neoformans* wild-type (W/T) and mutant (Mut) strains. BALB/c mice (five per group) were infected with 10^6 cells intratracheally, and organs were removed after 10 days of infection. Serial dilutions were plated to determine the number of yeast cells present in the tissue homogenates, expressed by CFU per gram of lung (D) or brain (E).

Mannitol is a potent inducer of *C. neoformans* capsule (41), and as the mutant strain is unable to transport it into the cell, it does not respond to the induction mediated by this polyol. Furthermore, the virulence of the strain lacking *PTP1* did not differ from that of the wild-type strain *in vitro*, in macrophages and amoeba, or *in vivo*, in mouse and *G. mellonella* models of infection. These results suggest that, despite its upregulation by *C. neoformans* inside phagocytic cells, disruption of this gene does not impair the establishment of fungal infection. The absence of an effect in virulence could be explained by the fact that 5- and 6-carbon polyols are unlikely to be sources of energy *in vivo*, since they have not been reported in animal tissues.

(ii) Genes related to *C. neoformans* metabolic adaptation to nutritional stress. Inside the phagosome, intracellular parasites adapt by modulating the expression of genes related to metabolic pathways. For example, the yeast *Candida albicans* modifies its metabolism to assimilate alternative carbon sources after phagocytosis by macrophages, which is reflected by the induction of the

gluconeogenesis, glyoxylate cycle, and β-oxidation pathways (35). Furthermore, *C. albicans* and *Paracoccidioides brasiliensis* show a strong reduction in the expression of genes involved in glycolysis in response to the glucose shortage inside the phagosome (35, 36). Similar patterns of expression were also observed for *C. neoformans* in response to the interaction with both host cells in this study. The switch from glycolysis to gluconeogenesis upon phagocytosis by amoebae and macrophages can be observed in the induction of the genes encoding the enzymes fructose-1,6-bisphosphatase (Fbp1) and phosphoenolpyruvate carboxykinase (Pck1), respectively. *C. neoformans* cells defective for the *PCK1* gene were avirulent in an animal model of infection (42).

The activation of the glyoxylate cycle is another important adaptation of many intracellular pathogens to the phagosomal microenvironment (34, 35, 43). Consistent with those observations, our results showed strong activation of the expression of its two regulatory enzymes, isocitrate lyase (Icl) and malate synthase (Mls), upon interaction of *C. neoformans* with both amoebae and macrophages. Additionally, our results suggest that acetyl coenzyme A (acetyl-CoA) generated from the oxidation of fatty acids drives the glyoxylate cycle. Transcripts related to enzymes of all steps of the *C. neoformans* β-oxidation pathway were induced upon internalization by amoebae and macrophages. Furthermore, genes related to peroxisome biogenesis, the organelle associated with cellular functions such as β-oxidation and hydrogen peroxide detoxification, were upregulated. Fatty acid oxidation is also required by other microorganisms after internalization by macrophages, such as *C. albicans* (35), and by *C. neoformans* in the lungs of infected mice (37). Taken together, our results show that *C. neoformans* cells responded similarly to nutritional stress within both amoebae and macrophages.

(iii) Genes related to oxidative/nitrosative stress and the electron transport chain. We identified seven and four *C. neoformans* genes related to the oxidative stress response that were upregulated after phagocytosis by *A. castellanii* and murine macrophages, respectively. Among them, the genes coding for catalases and cytochrome *c* peroxidase are of particular significance. *C. neoformans* has four genes that encode distinct catalases, and we showed that two of them were more expressed in response to the interaction with amoebae. Although it is proposed that catalases play an important role in the adaptation of the fungus to the intracellular environment of phagocytes, none of the four isoforms is required for virulence (44), probably due to the redundancy of the antioxidant system in *C. neoformans*. This may also explain why the enzyme cytochrome *c* peroxidase, which also acts in the detoxification of H_2O_2, has no role in the virulence of *C. neoformans* in mice (45). However, our results showed that its expression was induced after the interaction of the fungus with both hosts, in another case of disconnection between upregulation of gene expression in the presence of the host and role in virulence.

In addition to the oxidative stress, nitrosative stress acts as an antimicrobial mechanism by phagocytic cells. In *C. neoformans*, the enzyme thioredoxin reductase (Trr1) has been associated with protection from nitrosative stress (46), and we have found its gene upregulated upon phagocytosis by both cells, again suggesting that their microenvironments are similar.

Genes related to the electron transport chain were also modulated by both phagocytes. For example, the gene encoding cytochrome *c* oxidase (*COX1*) was downregulated in response to the interaction of *C. neoformans* with *A. castellanii*. Cox1 corresponds to the complex IV of the electron transport chain, reducing oxygen into water. This process is essential for cellular energy production but requires oxygen as the final acceptor of electrons. The intracellular environment presents *C. neoformans* with low levels of oxygen, which can explain the negative regulation of *COX1*. In agreement with our data, a hypoxic environment represses *COX1* expression in *Saccharomyces cerevisiae* (47). In contrast, there was no decrease in the *COX1* expression in macrophages, which may be explained by the fact that this gene is induced at 37°C (48). The evidence that both intracellular environments are low in oxygen was supported by the upregulation of the gene *FRD*, which encodes the enzyme fumarate reductase. This enzyme uses fumarate as the final acceptor of the electron transport chain, establishing an alternative pathway for energy generation in the absence of oxygen (49). In *Mycobacterium tuberculosis*, expression of FrdA from the fumarate reductase complex is induced in response to interaction with macrophages (34), and in *Mycobacterium phlei*, the activity of the Frd complex increases 4-fold when this bacterium is grown under oxygen restriction (50).

(iv) Genes related to thermal stress. Thermotolerance is critical for the virulence of human pathogens and the trehalose synthesis pathway is crucial for the infectivity of such pathogenic fungi as *C. albicans* (51, 52) and *C. neoformans* (53). In *C. neoformans*, the gene for trehalose synthase is induced at 37°C (54) and knockout strains of *C. neoformans* for the *TPS1* and *TPS2* genes, which encode trehalose-phosphate synthase and trehalose-phosphate phosphatase, respectively, are avirulent and unable to grow at 37°C (53). Curiously, our results showed that the *TPS1* gene is induced upon interaction of *C. neoformans* with amoebae at 25°C. Moreover, the Tps1 knockout strain of *C. neoformans* is less virulent in *Caenorhabditis elegans* at 25°C (53). These results suggest that the trehalose pathway may be involved in the response to stress conditions other than high temperature. In accordance with this, trehalose plays an important role in tolerance to desiccation (55) and hypoxia (56).

(v) Genes related to ergosterol. The biosynthesis of one molecule of ergosterol from squalene consumes 12 molecules of oxygen, which represents about 25% of the oxygen not used in the respiratory chain in *Saccharomyces cerevisiae* (57). Thus, it is expected that the concentration of oxygen in the environment affects ergosterol biosynthesis by fungi. Under hypoxic conditions, the concentration of ergosterol in the membrane of *S. cerevisiae* is only 25% of the concentration found in normoxia (58). Therefore, hypoxia in the intracellular environment of phagocytes may explain the downregulation of several genes related to ergosterol biosynthesis in *C. neoformans* after internalization by amoebae and macrophages.

(vi) Genes related to virulence. Steenbergen et al. (12) reported that strains defective in capsule synthesis and phospholipase B production were unable to survive inside amoebae, suggesting that they were required for persistence of the fungus in both mammalian and soil predator cells. In our experiments, we observed the induction of the genes *ISC1* and *CAP64*, which encode the enzyme C-inositol phosphosphingolipid phospholipase and a protein necessary for the synthesis of polysaccharide capsule, respectively, in response to *C. neoformans* internalization by *A. castellanii*. *ISC1* is important for *C. neoformans* survival within macrophages since it protects against nitrosative and oxidative stresses and the acidic pH found in the phagolysosome. Furthermore, *ISC1* is crucial for *C. neoformans* to spread to the central

nervous system (59). Likewise, *CAP64* seems to be important for *C. neoformans* virulence since knockout strains are avirulent (60). However, the precise function of *CAP64* in capsule formation is unknown (61). The upregulation of *ISC1* and *CAP64* by *C. neoformans* in response to *A. castellanii* suggests a convergence of adaptive mechanisms employed by this fungus to persist in amoebae and mammalian host cells.

Another gene of *C. neoformans* modulated in response to interaction with *A. castellanii* coded for the enzyme glucosylceramide synthase (Gcs). *GSC* is a pathogenesis regulator that ensures the growth of *C. neoformans* in neutral/alkaline pH and physiological concentrations of CO_2, a condition typically found in alveolar spaces. However, *GCS* has no involvement in fungal growth at acidic pH, as well as in fungal survival inside macrophages (62). In our microarray data, we found a decrease in the *GCS* transcript level after internalization of yeasts by *A. castellanii*, implying that this gene is not implicated in the persistence of *C. neoformans* inside amoebae either. Moreover, this result suggests that the intracellular environment of *A. castellanii* is acidic, as described for macrophages.

Overall, our results show that the transcriptional responses of *C. neoformans* to the hostile microenvironments of macrophages and amoebae are similar. The transcriptional profile in response to both phagocytes suggests an adaptive pattern to the stress of ingestion and phagosomal attack. The mechanisms of adaptation to phagocytic cells included the remodeling of central carbon metabolism, the expression of specific nutrient acquisition systems, and a response to the harsh conditions of the phagosome. Analysis of a highly expressed gene led to the identification and characterization of the *C. neoformans PTP1*. The fact that it was highly activated but irrelevant for murine or moth virulence is consistent with the notion that the transcriptional response to phagocytosis is a general stress response, which would necessarily include many genes that are not important in virulence. Although the transcriptional modulation of a specific gene of *C. neoformans* within phagocytic cells itself does not necessarily indicate a role in virulence, the comparative transcriptional profile provides insights into the adaptation of the fungus to key features of the host environment. In fact, the similarities between the transcriptional responses to ingestion by amoebae and macrophages are consistent with the view that cryptococcal virulence for mammals was selected by interactions with phagocytic predators in the environment and include adaptation to the intracellular milieu of eukaryotic phagocytic cells.

ACKNOWLEDGMENTS

We thank Mike Heinz and Seth Crosby from the Microarray Core Facility of the Washington University School of Medicine for technical assistance. We also thank André Nicola for relevant suggestions.

We thank CNPq and FAP/DF for financial support. L.S.D. was supported by a fellowship from CNPq. A.C. was supported by Public Health Service awards HL059842-3, A1033774, A1052733, and AI033142.

REFERENCES

1. **Ellis DH, Pfeiffer TJ.** 1990. Ecology, life cycle, and infectious propagule of *Cryptococcus neoformans*. Lancet **336**:923–925.
2. **Hogan LH, Klein BS, Levitz SM.** 1996. Virulence factors of medically important fungi. Clin. Microbiol. Rev. **9**:469–488.
3. **Alanio A, Desnos-Ollivier M, Dromer F.** 9 August 2011. Dynamics of *Cryptococcus neoformans*-macrophage interactions reveal that fungal background influences outcome during cryptococcal meningoencephalitis in humans. mBio **2**(4):e00158-11. doi:10.1128/mBio.00158-11.
4. **Fan W, Kraus PR, Boily MJ, Heitman J.** 2005. *Cryptococcus neoformans* gene expression during murine macrophage infection. Eukaryot. Cell **4**:1420–1433.
5. **Levitz SM, Nong SH, Seetoo KF, Harrison TS, Speizer RA, Simons ER.** 1999. *Cryptococcus neoformans* resides in an acidic phagolysosome of human macrophages. Infect. Immun. **67**:885–890.
6. **Feldmesser M, Kress Y, Novikoff P, Casadevall A.** 2000. *Cryptococcus neoformans* is a facultative intracellular pathogen in murine pulmonary infection. Infect. Immun. **68**:4225–4237.
7. **Casadevall A, Perfect JR.** 1998 *Cryptococcus neoformans*: molecular pathogenesis and clinical management. ASM Press, Washington, DC.
8. **Feldmesser M, Tucker S, Casadevall A.** 2001. Intracellular parasitism of macrophages by *Cryptococcus neoformans*. Trends Microbiol. **9**:273–278.
9. **Amer AO, Swanson MS.** 2002. A phagosome of one's own: a microbial guide to life in the macrophage. Curr. Opin. Microbiol. **5**:56–61.
10. **Lorenz MC, Fink GR.** 2002. Life and death in a macrophage: role of the glyoxylate cycle in virulence. Eukaryot. Cell **1**:657–662.
11. **Romanini L.** 2004. Immunity to fungal infections. Nat. Rev. Immunol. **4**:1–23.
12. **Steenbergen JN, Shuman HA, Casadevall A.** 2001. *Cryptococcus neoformans* interactions with amoebae suggest an explanation for its virulence and intracellular pathogenic strategy in macrophages. Proc. Natl. Acad. Sci. U. S. A. **98**:15245–15250.
13. **Steenbergen JN, Casadevall A.** 2003. The origin and maintenance of virulence for the human pathogenic fungus *Cryptococcus neoformans*. Microbes Infect. **5**:667–675.
14. **Casadevall A, Steenbergen JN, Nosanchuk JD.** 2003. 'Ready made' virulence and 'dual use' virulence factors in pathogenic environmental fungi—the *Cryptococcus neoformans* paradigm. Curr. Opin. Microbiol. **6**:332–337.
15. **Steenbergen JN, Nosanchuk JD, Malliaris SD, Casadevall A.** 2003. *Cryptococcus neoformans* virulence is enhanced after growth in the genetically malleable host *Dictyostelium discoideum*. Infect. Immun. **71**:4862–4872.
16. **Liu OW, Chun CD, Chow ED, Chen C, Madhani HD, Noble SM.** 2008. Systematic genetic analysis of virulence in the human fungal pathogen *Cryptococcus neoformans*. Cell **135**:174–188.
17. **Livak KJ, Schmittgen TD.** 2001. Analysis of relative gene expression data using real-time quantitative PCR and the $2^{-\Delta\Delta CT}$ method. Methods **25**:402–408.
18. **Kim MS, Kim SY, Yoon JK, Lee YW, Bahn YS.** 2009. An efficient gene-disruption method in *Cryptococcus neoformans* by double-joint PCR with NAT-split markers. Biochem. Biophys. Res. Commun. **390**:983–988.
19. **Toffaletti DL, Rude TH, Johnston SA, Durack DT, Perfect JR.** 1993. Gene transfer in *Cryptococcus neoformans* by use of biolistic delivery of DNA. J. Bacteriol. **175**:1405–1411.
20. **Nielsen K, Cox GM, Litvintseva AP, Mylonakis E, Malliaris SD, Benjamin DK, Jr, Giles SS, Mitchell TG, Casadevall A, Perfect JR, Heitman J.** 2005. *Cryptococcus neoformans* α strains preferentially disseminate to the central nervous system during coinfection. Infect. Immun. **73**:4922–4933.
21. **Chen SC, Wright LC, Santangelo RT, Muller M, Moran VR, Kuchel PW, Sorrell TC.** 1997. Identification of extracellular phospholipase B, lysophospholipase, and acyltransferase produced by *Cryptococcus neoformans*. Infect. Immun. **65**:405–411.
22. **Niehaus WG, Flynn T.** 1994. Regulation of mannitol biosynthesis and degradation by *Cryptococcus neoformans*. J. Bacteriol. **176**:651–655.
23. **Feldmesser M, Casadevall A.** 1997. Effect of serum IgG1 to *Cryptococcus neoformans* glucuronoxylomannan on murine pulmonary infection. J. Immunol. **158**:790–799.
24. **García-Rodas R, Casadevall A, Rodríguez-Tudela JL, Cuenca-Estrella M, Zaragoza O.** 2011. *Cryptococcus neoformans* capsular enlargement and cellular gigantism during *Galleria mellonella* infection. PLoS One **6**:e24485. doi:10.1371/journal.pone.0024485.
25. **Ma H, Croudace JE, Lammas DA, May RC.** 2006. Expulsion of live pathogenic yeast by macrophages. Curr. Biol. **16**:2156–2160.
26. **Alvarez M, Casadevall A.** 2006. Phagosome extrusion and host-cell survival after *Cryptococcus neoformans* phagocytosis by macrophages. Curr. Biol. **16**:2161–2165.
27. **Zaragoza O, Chrisman CJ, Castelli MV, Frases S, Cuenca-Estrella M, Rodríguez-Tudela JL, Casadevall A.** 2008. Capsule enlargement in *Cryptococcus neoformans* confers resistance to oxidative stress suggesting a mechanism for intracellular survival. Cell. Microbiol. **10**:2043–2057.

28. **Casadevall A.** 2012. Amoeba provides insight into the origin of virulence in pathogenic fungi. Adv. Exp. Med. Biol. **710**:1–10.
29. **Bunting LA, Neilson JB, Bulmer GS.** 1979. *Cryptococcus neoformans*: gastronomic delight of a soil ameba. Sabouraudia **17**:225–232.
30. **Ruiz A, Neilson JB, Bulmer GS.** 1982. Control of *Cryptococcus neoformans* in nature by biotic factors. Sabouraudia **20**:21–29.
31. **Chrisman CJ, Albuquerque P, Guimaraes AJ, Nieves E, Casadevall A.** 2011. Phospholipids trigger *Cryptococcus neoformans* capsular enlargement during interactions with amoebae and macrophages. PLoS Pathog. **7**:e1002047. doi:10.1371/journal.ppat.1002047.
32. **Rahme LG, Tan MW, Le L, Wong SM, Tompkins RG, Calderwood SB, Ausubel FM.** 1997. Use of model plant hosts to identify *Pseudomonas aeruginosa* virulence factors. Proc. Natl. Acad. Sci. U. S. A. **94**:13245–13250.
33. **Lorenz MC, Fink GR.** 2001. The glyoxylate cycle is required for fungal virulence. Nature **412**:83–86.
34. **Schnappinger D, Ehrt S, Voskuil MI, Liu Y, Mangan JA, Monahan IM, Dolganov G, Efron B, Butcher PD, Nathan C, Schoolnik GK.** 2003. Transcriptional adaptation of *Mycobacterium tuberculosis* within macrophages: insights into the phagosomal environment. J. Exp. Med. **198**:693–704.
35. **Lorenz MC, Bender JA, Fink GR.** 2004. Transcriptional response of *Candida albicans* upon internalization by macrophages. Eukaryot. Cell **3**:1076–1087.
36. **Tavares AH, Silva SS, Dantas A, Campos EG, Andrade RV, Maranhão AQ, Brígido MM, Passos-Silva DG, Fachin AL, Teixeira SM, Passos GA, Soares CM, Bocca AL, Carvalho MJ, Silva-Pereira I, Felipe MS.** 2007. Early transcriptional response of *Paracoccidioides brasiliensis* upon internalization by murine macrophages. Microbes Infect. **9**:583–590.
37. **Hu G, Cheng PY, Sham A, Perfect JR, Kronstad JW.** 2008. Metabolic adaptation in *Cryptococcus neoformans* during early murine pulmonary infection. Mol. Microbiol. **69**:1456–1475.
38. **Onishi H, Suzuki T.** 1968. Production of D-mannitol and glycerol by yeasts. Appl. Microbiol. **16**:1847–1852.
39. **Wong B, Perfect JR, Beggs S, Wright KA.** 1990. Production of the hexitol D-mannitol by *Cryptococcus neoformans in vitro* and in rabbits with experimental meningitis. Infect. Immun. **58**:1664–1670.
40. **Chaturvedi V, Flynn T, Niehaus WG, Wong B.** 1996. Stress tolerance and pathogenic potential of a mannitol mutant of *Cryptococcus neoformans*. Microbiology **142**:937–943.
41. **Guimarães AJ, Frases S, Cordero RJ, Nimrichter L, Casadevall A, Nosanchuk JD.** 2010. *Cryptococcus neoformans* responds to mannitol by increasing capsule size *in vitro* and *in vivo*. Cell. Microbiol. **12**:740–753.
42. **Panepinto J, Liu L, Ramos J, Zhu X, Valyi-Nagy T, Eksi S, Fu J, Jaffe HA, Wickes B, Williamson PR.** 2005. The DEAD-box RNA helicase Vad1 regulates multiple virulence associated genes in *Cryptococcus neoformans*. J. Clin. Invest. **115**:632–641.
43. **Derengowski LS, Tavares AH, Silva S, Procópio LS, Felipe MS, Silva-Pereira I.** 2008. Upregulation of glyoxylate cycle genes upon *Paracoccidioides brasiliensis* internalization by murine macrophages and *in vitro* nutritional stress condition. Med. Mycol. **46**:125–134.
44. **Giles SS, Stajich JE, Nichols C, Gerrald QD, Alspaugh JA, Dietrich F, Perfect JR.** 2006. The *Cryptococcus neoformans* catalase gene family and its role in antioxidant defense. Eukaryot. Cell **5**:1447–1459.
45. **Giles SS, Perfect JR, Cox GM.** 2005. Cytochrome c peroxidase contributes to the antioxidant defense of *Cryptococcus neoformans*. Fungal Genet. Biol. **42**:20–29.
46. **Missall TA, Lodge JK.** 2005. Thioredoxin reductase is essential for viability in the fungal pathogen *Cryptococcus neoformans*. Eukaryot. Cell **4**:487–489.
47. **Dagsgaard C, Taylor LE, O'Brien KM, Poyton RO.** 2001. Effects of anoxia and the mitochondrion on expression of aerobic nuclear COX genes in yeast: evidence for a signaling pathway from the mitochondrial genome to the nucleus. J. Biol. Chem. **276**:7593–7601.
48. **Toffaletti DL, Del Poeta M, Rude TH, Dietrich F, Perfect JR.** 2003. Regulation of cytochrome c oxidase subunit 1 (*COX1*) expression in *Cryptococcus neoformans* by temperature and host environment. Microbiology **149**:1041–1049.
49. **Li AH, Lam WL, Stokes RW.** 2008. Characterization of genes differentially expressed within macrophages by virulent and attenuated *Mycobacterium tuberculosis* identifies candidate genes involved in intracellular growth. Microbiology **154**:2291–2303.
50. **Gillespie J, Barton LL, Rypka EW.** 1988. Influence of oxygen tension on the respiratory activity of *Mycobacterium phlei*. J. Gen. Microbiol. **134**:247–252.
51. **Gancedo C, Flores CL.** 2004. The importance of a functional trehalose biosynthetic pathway for the life of yeasts and fungi. FEMS Yeast Res. **4**:351–359.
52. **Zaragoza O, de Virgilio C, Pontón J, Gancedo C.** 2002. Disruption in *Candida albicans* of the TPS2 gene encoding trehalose-6-phosphate phosphatase affects cell integrity and decreases infectivity. Microbiology **148**:1281–1290.
53. **Petzold EW, Himmelreich U, Mylonakis E, Rude T, Toffaletti D, Cox GM, Miller JL, Perfect JR.** 2006. Characterization and regulation of the trehalose synthesis pathway and its importance in the pathogenicity of *Cryptococcus neoformans*. Infect. Immun. **74**:5877–5887.
54. **Kraus PR, Boily MJ, Giles SS, Stajich JE, Allen A, Cox GM, Dietrich FS, Perfect JR, Heitman J.** 2004. Identification of *Cryptococcus neoformans* temperature-regulated genes with a genomic-DNA microarray. Eukaryot. Cell **3**:1249–1260.
55. **Hottiger T, Boller T, Wiemken A.** 1987. Rapid changes of heat and desiccation tolerance correlated with changes of trehalose content in *Saccharomyces cerevisiae* cells subjected to temperature shifts. FEBS Lett. **220**:113–115.
56. **Chen Q, Haddad GG.** 2004. Role of trehalose phosphate synthase and trehalose during hypoxia: from flies to mammals. J. Exp. Biol. **207**:3125–3129.
57. **Rosenfeld E, Beauvoit B.** 2003. Role of the non-respiratory pathways in the utilization of molecular oxygen by *Saccharomyces cerevisiae*. Yeast **20**:1115–1144.
58. **Shobayashi M, Mitsueda S, Ago M, Fujii T, Iwashita K, Iefuji H.** 2005. Effects of culture conditions on ergosterol biosynthesis by *Saccharomyces cerevisiae*. Biosci. Biotechnol. Biochem. **69**:2381–2388.
59. **Shea JM, Kechichian TB, Luberto C, Del Poeta M.** 2006. The cryptococcal enzyme inositol phosphosphingolipid-phospholipase C confers resistance to the antifungal effects of macrophages and promotes fungal dissemination to the central nervous system. Infect. Immun. **74**:5977–5988.
60. **Wilder JA, Olson GK, Chang YC, Kwon-Chung KJ, Lipscomb MF.** 2002. Complementation of a capsule deficient *Cryptococcus neoformans* with CAP64 restores virulence in a murine lung infection. Am. J. Respir. Cell Mol. Biol. **26**:306–314.
61. **Chang YC, Penoyer LA, Kwon-Chung KJ.** 1996. The second capsule gene of *Cryptococcus neoformans*, *CAP64*, is essential for virulence. Infect. Immun. **64**:1977–1983.
62. **Rittershaus PC, Kechichian TB, Allegood JC, Merrill AH, Jr, Hennig M, Luberto C, Del Poeta M.** 2006. Glucosylceramide synthase is an essential regulator of pathogenicity of *Cryptococcus neoformans*. J. Clin. Invest. **116**:1651–1659.